Review

Advanced Electrical Machines and Machine-Based Systems for Electric and Hybrid Vehicles

Ming Cheng [1],*, Le Sun [1], Giuseppe Buja [2] and Lihua Song [1]

[1]   School of Electrical Engineering, Southeast University, Nanjing 210096, China;
      E-Mails: sunle1987@live.cn (L.S.); songlihua0418@163.com (L.S.)

[2]   Department of Industrial Engineering, University of Padova, Padova 35131, Italy;
      E-Mail: giuseppe.buja@unipd.it

*   Author to whom correspondence should be addressed; E-Mail: mcheng@seu.edu.cn;
      Tel.: +86-25-8379-4152; Fax: +86-25-8379-1696.

Abstract: The paper presents a number of advanced solutions on electric machines and machine-based systems for the powertrain of electric vehicles (EVs). Two types of systems are considered, namely the drive systems designated to the EV propulsion and the power split devices utilized in the popular series-parallel hybrid electric vehicle architecture. After reviewing the main requirements for the electric drive systems, the paper illustrates advanced electric machine topologies, including a stator permanent magnet (stator-PM) motor, a hybrid-excitation motor, a flux memory motor and a redundant motor structure. Then, it illustrates advanced electric drive systems, such as the magnetic-geared in-wheel drive and the integrated starter generator (ISG). Finally, three machine-based implementations of the power split devices are expounded, built up around the dual-rotor PM machine, the dual-stator PM brushless machine and the magnetic-geared dual-rotor machine. As a conclusion, the development trends in the field of electric machines and machine-based systems for EVs are summarized.

Keywords: permanent magnet machine; hybrid-excitation; memory motor; fault-tolerant control; power split; electric variable transmission; hybrid vehicles; electric vehicle

1. Introduction

In recent decades, the rapid increase in the amount of vehicles in use has seriously impacted on worldwide energy consumption and environment. Compared to the internal combustion engine (ICE) vehicles (ICEV), electric vehicles (EVs) contribute significantly to the energy saving and environmental protection, and on account of these benefits, they constitute today's direction for the automotive industry.

EVs are vehicles wholly- or partially-driven by electricity. Specifically, they are battery-powered electric vehicles (BEVs), fuel cell electric vehicles (FEVs) and hybrid electric vehicles (HEVs) [1]. A basic classification of EVs is shown in Figure 1. In a globalized automotive market, the major vehicle manufactures have launched their own commercial EV products, such as Toyota Prius, Toyota Mirai, GM Volt, Nissan Leaf, and so on. In addition, non-traditional vehicle companies, such as Tesla and Google, have also entered into the EV market and have launched a series of distinctive EV products.
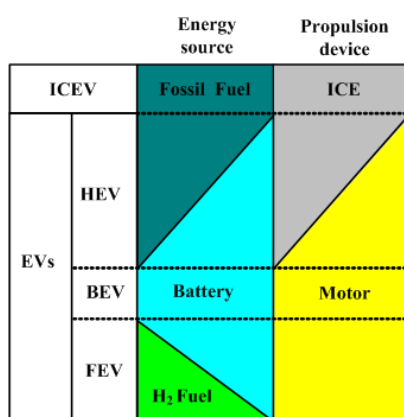

Figure 1. EV classification. ICEV, internal combustion engine vehicle; HEV, hybrid electric vehicle; BEV, battery-powered electric vehicle; FEV, fuel cell electric vehicle.

Different from the ICE vehicles, EVs have an electric motor embedded in the powertrain. Since the efficiency in the energy conversion of an electric motor together with the associated power electronics supply is much higher than ICEs, EVs need less energy to move. Furthermore, exploiting the capabilities of the electric motors, additional abatement in energy consumption can be achieved. For instance, the start-stop and the regenerative braking features can further reduce the energy consumption by approximately 20%–30%. Therefore, EVs are convenient, not only for increasing the efficiency in the energy utilization, but also for cutting out environmental pollution in an equal proportion.

Batteries, electric machines, electric drive systems and individual mechanical devices are the key technologies of an EV/HEV powertrain. In particular, the electric drive systems propelling the vehicles are the heart of any EV, and their operation directly affects the overall EV performance. Besides, individual mechanical devices, like the power split, play a crucial role in HEVs with the popular series-parallel architecture, and their operation directly influences the achievement of the driving efficiency goals.

The purpose of this paper is to present a number of advanced solutions on electric machines, electric drive systems and the implementation of the power split devices by means of electric machines. In detail, the paper is organized as follows. Section 2 reviews the main requirements for the electric drive systems designated to the EV propulsion. Sections 3 and 4 illustrate advanced electric

machine topologies and drive systems, including stator a permanent magnet (PM) motor, a hybrid-excitation motor, a flux memory motor, an in-wheel motor drive and an integrated starter generator (ISG). Section 5 expounds three advanced implementations of the power split devices for HEVs, built around machine-based systems that use the dual-rotor PM machine, the dual stator PM brushless machine and the magnetic-geared dual-rotor brushless machine (MGDRM), respectively. Section 6 provides an outlook of the development trends in the field of electric machines and machine-based systems for EVs. Section 7 closes the paper.

2. Electric Vehicle Drive System

The peculiar operating modes and working conditions of vehicles pose specific requirements for the electric motors and drive systems to be used in an EV's powertrain. This has pushed academics all over the world to regard EV motors and drive systems as a special category. The main differences between EV motors and conventional industrial motors are listed in Table 1, whilst the main requirements for the EV drive systems are as follows [2–4]:

(1) High torque density and power density.
(2) Very wide speed range, for example the speed range of the constant power region should be 3–4-times that of the constant torque region, as shown in Figure 2.
(3) Extended area of high efficiency; it should cover most of the operating regions.
(4) Large torque output at low speeds in order to dispose of enough torque when the vehicle starts or is climbing.
(5) Strong overload capability, for instance the motor can output two-times the rated torque during a short time.
(6) Security and reliability, for instance fault-tolerant configurations should be arranged.
(7) Motor noise and torque ripple should be suppressed.
(8) Reasonable costs.

Table 1. Comparison of EV motors and traditional industrial motors.

| Items	EV motors	Traditional industrial motors
Ambient temperate	−40~140 °C	20~40 °C
Operation environment	Adverse	Indoor
Coolant temperate	75~150 °C	<40 °C
Winding temperate	160~200 °C	75~130 °C
Speed range	0~15,000 rpm	<3000 rpm
Noise level	Very low	Low
Speed demand	Frequent changes	Keep uniform
Installation space	Very limited	Loose
System voltage	Independent/Variable	Static grid
Efficiency	Efficient	Determined by application
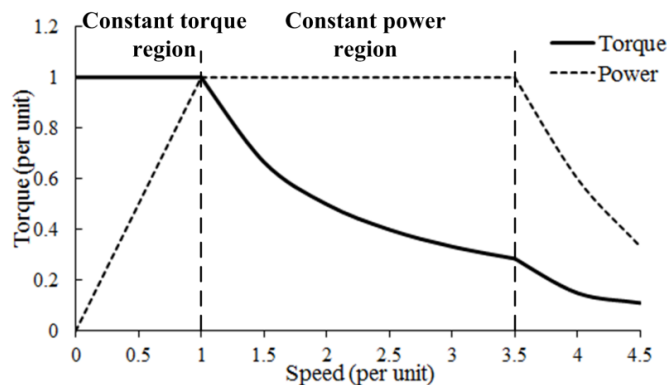
Figure 2. Torque and power requirements for the electric drive systems [4].

Induction machines (IM), switched reluctance machines (SRM) and permanent magnet synchronous machines (PMSM) are standard motor topologies in current electric drive systems. Typical structures of the three kinds of motor are shown in Figure 3, and a comparison of their main data is listed in Table 2 [5].
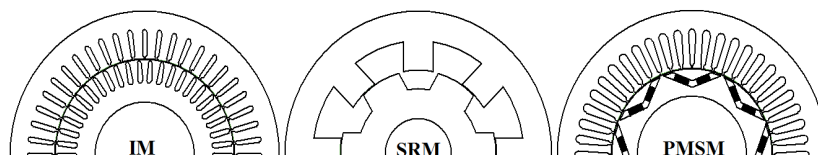

Figure 3. Three popular motors in EV: Induction machines (IM), switched reluctance machines (SRM) and permanent magnet synchronous machines (PMSM).

Table 2. Comparison of three kinds of motors.

Motor type	Torque (Nm)	Armature current density (A/mm^2)	Efficiency (%)
		1500 r/min	
PMSM(Prius)	303	15.7	91.3
SRM	297	15.8/12.1	83.1
IM	294	20.1	85.2
		6000 r/min	
PMSM(Prius)	45.6	3.75	96.1
SRM	50.8	4.51/3.72	95.2
IM	52.1	4.02	88.2

As shown in Table 2, the efficiency of PMSM is higher than IM and SRM. Moreover, since the control of IM is more complex and the torque ripple of SRM is more conspicuous, PMSM has become a common solution for EV motors. However, traditional PM motors have their intrinsic weaknesses. For instance, cooling the magnets mounted in the rotor is difficult because of the poor thermal dissipation, especially in HEVs, since the motor is positioned close to the ICE.

In recent years, to overcome the drawbacks of the traditional PM motors for EV applications, new motor topologies, lay-out schemes and control methods have been researched. The results of the research have opened non-explored ways towards the development of novel EVs. Hereafter, an overview of some of the latest PM machines and PM machine-based systems for EVs is given.

3. Advanced Motor Topologies

3.1. Stator Permanent Magnet Motor

According to the location of the magnets installed in the PM motors, they can be divided into rotor-PM motor and stator-PM motor. Rotor-PM motors are now widely used in applications; however, as previously mentioned, they are subjected to high heating stresses, which cause PM irreversible demagnetization and impairment of the power output, thereby reducing the power density. Furthermore, rotor-PM motors need special auxiliary measures to overcome the centrifugal forces at high speeds, which yield complex structures and high manufacturing costs. In recent years, stator-PM motors, *i.e.*, motors with the magnets mounted in the stator, have attracted much attention, as they are deemed a promising solution to overcome the shortcomings of the rotor-PM motors [6].

Figure 4 illustrates two representative topologies of stator-PM motors: doubly-salient PM motor (DSPM) and flux switching PM motor (FSPM).
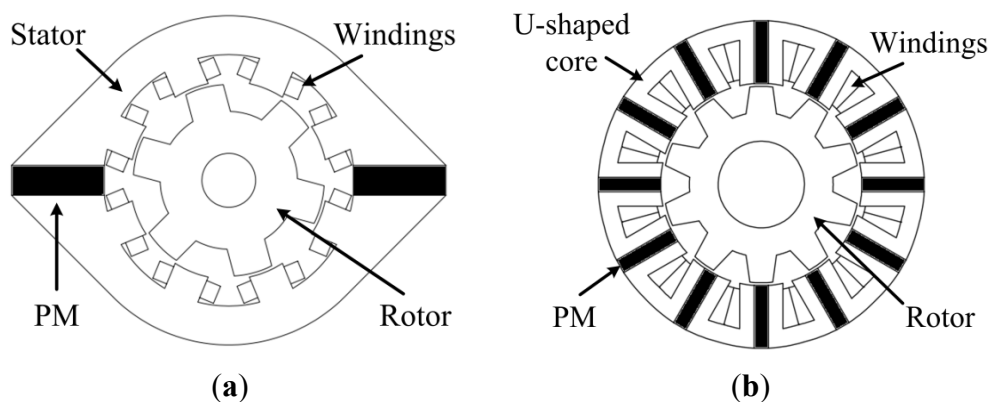

Figure 4. Two representative stator-permanent magnet (PM) motor topologies. (**a**) Doubly-salient PM motor (DSPM); (**b**) Flux switching PM motor (FSPM).

3.1.1. Doubly-Salient PM Motor (DSPM)

DSPM [7,8] is the simplest structure of stator-PM motor. In essence, DSPM can be considered as a combination of SRM and stator magnets, as shown in Figure 4a. The structure has concentrated windings wound around the stator expansions and magnets inserted into the stator back-core, making the flux produced by the magnets and linked to the windings unipolar. When the salient-pole rotor revolves, the flux path varies. Under no-load conditions, the flux linked to the windings alternatively increases and decreases linearly, and the back-electromotive force EMF induced in the windings is trapezoidal.

Since the flux linkage in a DSPM is unipolar, the torque density is relatively lower than in motors with bipolar flux linkage. Additionally, to get a sinusoidal back-EMF and to obtain a low output torque ripple, skewing of the pole is required [9], leading to a reduction of the average torque output. However, in addition to having a simple and reliable structure, this motor topology uses less magnets, so that it can cost less than other stator-PM motors and generates a torque per PM mass unit higher than any other structure.

Power-sizing equations of DSPM have been derived in [9,10] and provide the designer with a useful tool for the preliminary evaluation of the motor dimensions. A nonlinear time-varying magnetic circuit describing the DSPM behavior was built in [11] and allows an effective investigation of the DSPM electromagnetic performance. The loss model of rotor-PM motors is somewhat different from stator-PM motors due to the DC-biased magnetic induction. Further to this difference, a proper loss analysis for DSPM was carried out in [12,13] by working out a method that is also applicable to other stator-PM motors.

3.1.2. Flux Switching PM Motor (FSPM)

As shown in Figure 4b, the stator of a FSPM consists of U-shaped core units and an equal number of magnets, each of them sandwiched between two core units. The magnets are magnetized circumferentially and alternatively in opposite directions. The rotor has ten salient poles without magnets and windings. Concentrated windings are wound around two adjacent stator teeth, which makes the flux produced by the magnets and linked to the windings bipolar [14].

FSPM has winding consistency and complementarity [15]. Due to the difference in the magnetic reluctance between the two pairs of windings composing a phase, the flux-linkage and the no-load back-EMF induced in the windings are nearly sinusoidal, as shown in Figure 5. Therefore, an FSPM is suited to operate as a brushless AC (BLAC) motor. In order to make the torque ripple of an FSPM even more negligible, appropriate designs of both the rotor structure [16] and the motor control algorithm [17] have been also devised.
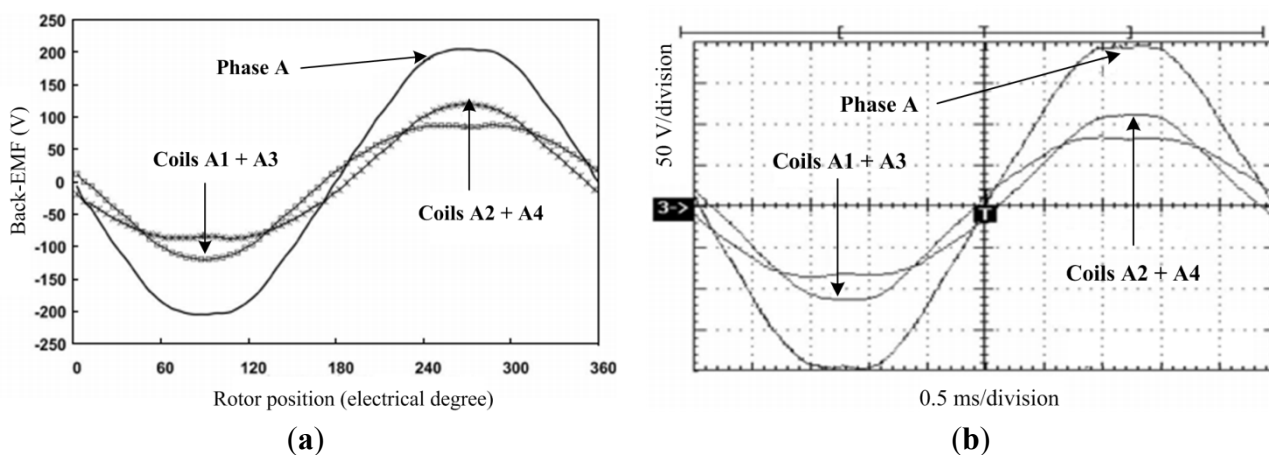

Figure 5. Coils and phase EMF waveforms of a 12/10-pole FSPM machine: (**a**) Predicted; (**b**) Measured.

Additionally, the features of concentrated windings, intrinsic modular stator and simple rotor saliencies make the FSPM manufacturing easy (as shown in Figure 6). Therefore, FSPM is a potential candidate for the mass production of the automobile industry.
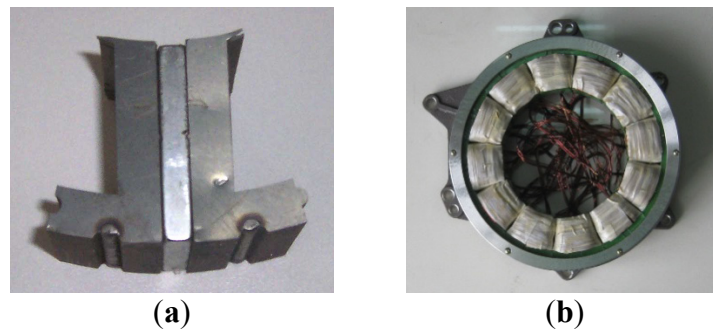
(a) (b)

Figure 6. One module (**a**) and the assembly (**b**) of the stator.

Like for DSPM, power-sizing equations of FSPM have been derived in [18,19] and provide the designer with a useful tool for the preliminary evaluation of the motor dimensions. Influences of the rotor pole number, slot opening and winding configuration on the motor characteristics have been discussed in [20–22]. A nonlinear time-varying magnetic circuit describing the FSPM behavior was built in [23] and allows an effective investigation of the DSPM electromagnetic performance. Quantitative assessment of FSPM performance against that of the traction motor of the Prius 2004 (interior-PM motor) has been conducted in [24], finding that the torque per volume of FSPM can match the counterpart of the interior PM (IPM) motor and that the torque ripple of FSPM is less than that of the IPM motor.

Compared to the rotor-PM motor, the stator-PM motor not only takes advantage of the mechanical structure and the magnets' cooling, but also introduces the important philosophy of placing the flux excitation source on the stator. Such a philosophy originated a series of novel and useful motor typologies for EV drive systems.

3.2. Hybrid-Excitation Motor

When vehicles cruise at high speeds, traditional PM motors use the direct axis current component to operate the flux-weakening [25], *i.e.*, to compensate for the uncontrollable PM flux. However, flux weakening suffers from some limitations, especially in PM motors with low direct axis inductance [26]. Hybrid-excitation motors refer to PM motors for which their magnetic field is established by both the field windings and the permanent magnets [27]. Hence, a flexible flux control can be achieved thanks to the field windings. Explicitly, the large torque requirement at low speeds can be satisfied by supplying the field windings with a positive current that strengthens the flux, whilst the constant-power requirement at high speeds can be obtained by supplying the field windings with a negative current that weakens the flux [28].

Figure 7 shows a type of hybrid-excitation DSPM motor (HEDS) [29]. HEDS fully exploits the unique advantage of the stator-PM motor of mounting the magnets only in the stator, by using a DC field winding, still placed on the stator, to achieve flux control. Together with flux control, optimization of the motor efficiency is obtained over a wide speed range, especially at high speeds [30]. The measured efficiency-speed characteristic of HEDS without and with flux control is depicted in Figure 8. As expected, the flux regulation greatly improves the motor efficiency in the high speed range.

Similar to the principle of HEDS, the hybrid excitation FSPM motor (HEFS) has been also proposed in [31], as shown in Figure 9. The DC field windings, which are placed in the stator, can effectively regulate the motor flux [32]. Details of the flux-regulation theory of HEFS are given in [33].
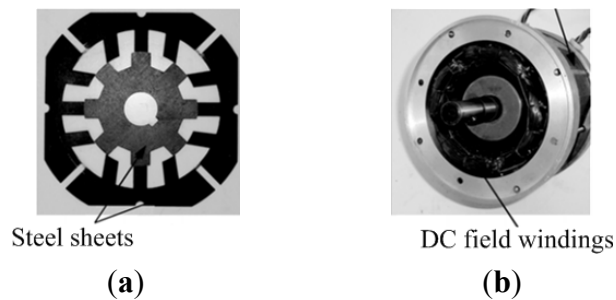
Steel sheets   DC field windings

(**a**)   (**b**)

Figure 7. Hhybrid-excitation DSPM motor (HEDS) (**a**) Steel sheets; (**b**) Assembly of the HEDS.
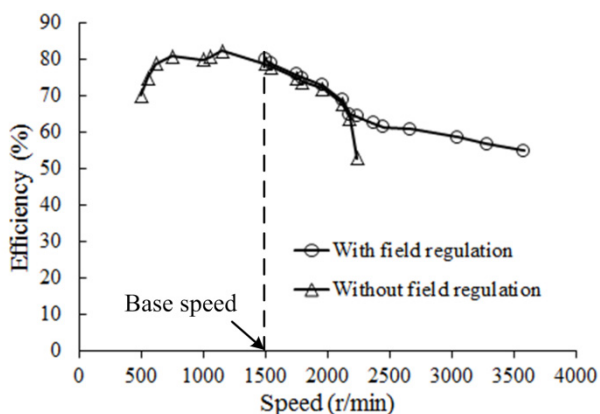

Figure 8. The effect of DC field regulation on the motor efficiency.

HEFS inherits the advantages of the FSPM motor, namely the bipolar flux linkage, the sinusoidal back-EMF waveform and the easy modular manufacturing; furthermore, it has the merits of a simple flux control and a remarkable efficiency for operation at high speeds.
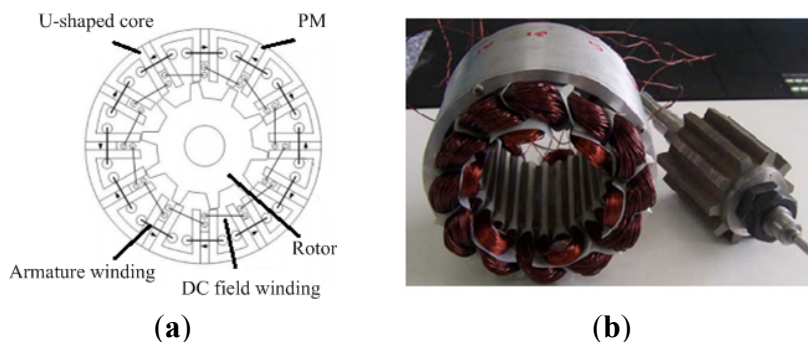

(**a**)   (**b**)

Figure 9. HEFS motor. (**a**) Schematic; (**b**) Prototype.

3.3. Flux Memory Motor

The field winding operation of the hybrid excitation motor is simple and reliable, but the DC excitation current flowing in the field winding inevitably increases the coil losses when field regulation is needed. In order to overcome such a drawback, special permanent magnets having high remanence, but low coercive force (such as AlNiCo magnets) can be used. Indeed, by taking the chance that they offer of changing their magnetization state by a current pulse, the flux produced by these magnets in

the motor can be easily adjusted by entering a current pulse into the field winding. Additionally, the change of the magnetization state is immediate and can be held on by the magnets; for this reason, the magnets are termed as "memory" magnets and the motors set up with these magnets as "flux memory motors" [34]. Although the flux in a flux memory motor can be regulated by a current pulse, the need remains to excite the field winding. However, the current pulse is transient, so the coil losses are negligible.

The memory magnet technology can be combined with the stator-PM motor for adjusting the flux in the machine [35–37]. Of course, a stator-PM motor can utilize the existing DC field winding placed on the stator to magnetize or demagnetize the magnets. Worth noting, this solution is simpler and more efficient than the traditional flux weakening of the rotor-PM motors. Figure 10a illustrates a DSPM memory motor.
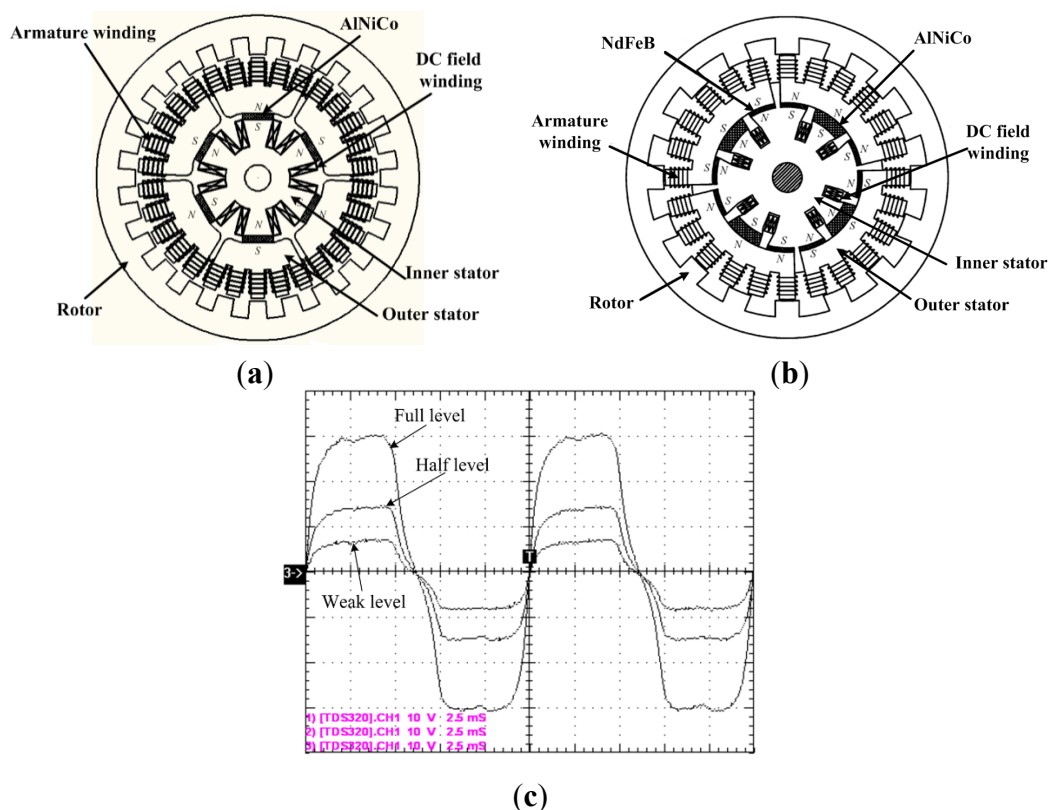

Figure 10. Stator-PM memory motor. (**a**) DSPM memory motor; (**b**) DSPM memory motor with NdFeB and AlNiCo; (**c**) No-load back-EMF at different PM flux levels.

The drawback of a memory motor is that the remanence of the memory magnets is relatively less than common magnets (such as NdFeB magnets). Hence, the power density is also less. A higher power density can be obtained by the novel structure proposed in [38] for a memory DSPM. The structure contains both AlNiCo and NdFeB magnets, as shown in Figure 10b. The NdFeB magnets, having a high remanence, help the memory motor to achieve a better power density, while they do not impair the flux regulation capability of the motor. Figure 10c shows the back-EMF waveforms of a memory DSPM for different magnetizing levels. Because of these properties, the memory stator-PM motor appears to be a very convenient solution for EV applications with operation over a wide speed range.

3.4. Redundant Structure and Fault-Tolerance Control

For an EV to be reliable, it is mandatory to arrange a fault-tolerant powertrain. Hence, the issue of PM motors with fault-tolerant capabilities has become more and more important [39].

Four-phase DSPM has the innate feature of fault-tolerance [40]. In cases of a short-circuit fault, an open-circuit fault and an inverter fault, by reconfiguring the drive system and adapting the motor control [41], torque output can be kept at a relatively high level.

Arranging a redundant structure for the motors is a widely-used means to cope with a fault. An FSPM with a redundant structure (R-FSPM) is shown in Figure 11 [42]. Its windings are divided into two groups, which are supplied by two independent inverters. By this structure, if an open-circuit fault happens on one of the phase windings, the average torque developed by the R-FSPM can be preserved by increasing the current in the healthy windings [42]. Additionally, by utilizing the harmonic current injection method [43], the needed current can be reduced with no average torque reduction or severe torque ripple.
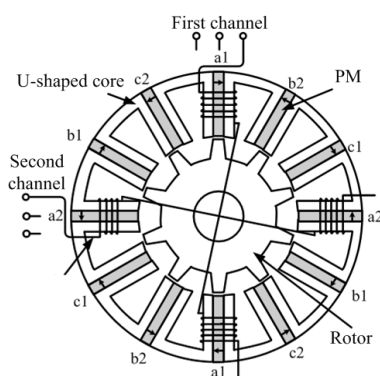

Figure 11. FSPM redundant structure.

The straight forward approach to make a motor tolerant to a phase fault is to maintain it operation by the help of the remaining healthy phases. Hence, the more motor phases there are, the better the motor behavior is under a phase fault. As a result, multi-phase motors, as a common setup of redundant structures, have gained great importance in a motor design intended for the fault-tolerance. The works in [44,45] have given a systematic review of the multiphase electric machines and control strategies. Based on the stator-PM motors, for instance, a nine-phase FSPM is shown in Figure 12 [46].
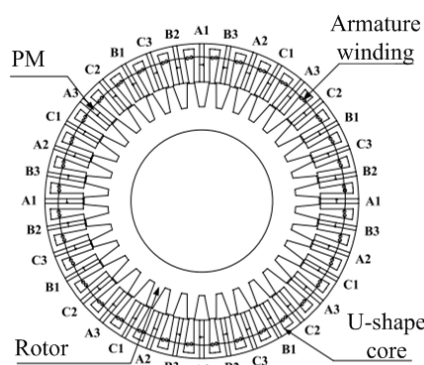

Figure 12. Nine-phase FSPM for a fault-tolerance application.

By controlling the motor with an algorithm developed on purpose to tolerate the fault, the nine-phase motor can operate under open-circuit fault conditions with no average torque reduction [47]. The torque waveform with the fault-tolerant control is traced in Figure 13. As the figure highlights, the phase open-circuit fault occurs at 20 ms and the torque ripple deteriorates; at 30 ms, when the fault-tolerant control is activated, average torque and torque ripple are somewhat the same as before the fault.

In conclusion, a redundant structure and a fault-tolerant control make the motors operational even in spite of a fault, thereby improving trustworthiness and safety in EV driving.
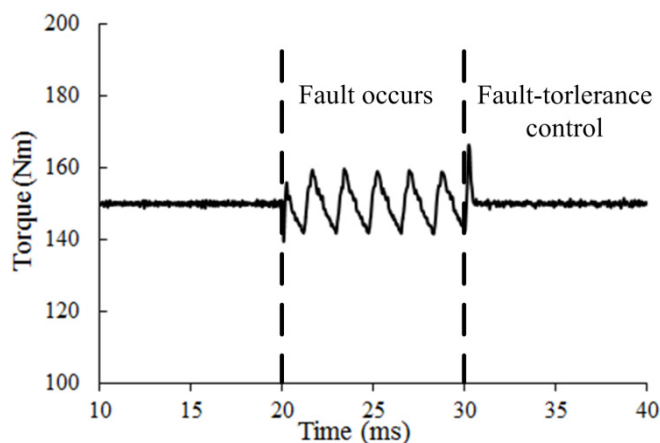

Figure 13. Torque output of the nine-phase FSPM fault-tolerant control.

The key features of the aforementioned motor topologies are summarized in Table 3.

Table 3. Comparison of different motor topologies.

Motor topology	Stator-PM motors			Hybrid-excitation motor	Flux memory motor
	DSPM	FSPM	FRPM		
Stator	Salient poles with both PM and armature windings				
Rotor	Salient poles with neither magnets nor windings				
Magnet location	Stator				
Magnet volume	Low	Medium	High	Lower than PM counterpart	Similar to PM counterpart
Magnet material	NdFeB	NdFeB	NdFeB	NdFeB	AlNiCo
Field winding	-	-	-	Stator	Stator
Field coil loss	-	-	-	High	Negligible
Flux controllability	Low	Low	Low	High	High
Speed range	Limited	Limited	Limited	Wide	Wide
Torque Density	Low	Low	High	Medium	Medium

4. Advanced Electric Drive System

In recent years, the performance improvement of a single electric machine has not satisfied the demands posed by the modern EV powertrain. Integrated electric drive systems for vehicle propulsion have been considered as a promising way of satisfying these demands. In this section, two integrated electric drive systems for the EV powertrain technologies, namely the magnetic-geared in-wheel drive system and the integrated stator generator (ISG), are illustrated.

4.1. Magnetic-Geared In-Wheel Drive System

The in-wheel drive system can make a more accurate torque distribution to the four wheels of a vehicle, and such an achievement does not depend on the gear box, drive axle or differential mechanism. Therefore, the in-wheel drive system can greatly reduce the complexity and mass of the vehicles. Additionally, the in-wheel drive system can also reduce the turning radius of vehicles, which makes steering more manageable. Although the in-wheel drive system has so many merits, the torque density of the traditional motor limits its application. This is because the rotation speed of a wheel is not high (such as 600 r/min), while it needs a relatively large torque, as is typical for a "low speed large torque (LSLT)" application. The conventional solution for this application is the planetary gear speed reduction element, but the usage of mechanical gears causes transmission loss and noise and requires a lubrication system.

The magnetic-geared in-wheel drive system is an electric drive system that implements the LSLT operation by a coaxial magnetic gear. The magnetic gear is attractive for an in-wheel system, as it does the gearing function without any mechanical gear. The functioning of a coaxial magnetic gear can be explained by the magnetic field modulation used to transmit the torque between two rotors with different pole numbers [48]. The speeds of the two rotors can be expressed as:

$$p_{in} \times n_{in} = p_{out} \times n_{out} \tag{1}$$

where p_{in} and n_{in} are the pole pair number and rotation speed of the inner rotor, respectively, and p_{out} and n_{out} are the pole pair number and rotation speed of the outer rotor, respectively. Complementing Equation (1) with the equation that states the power invariance, the relationship between the inner and outer rotor torques is readily obtained.

Compared to the mechanical gear, the torque transmission of the magnetic gear has no contact, thus avoiding any abrasion of the in-contact parts or mechanical noise. Additionally, the magnetic gear itself has overload protection ability [49]. Figure 14a shows the basic structure of a coaxial magnetic gear. By simply integrating the coaxial magnetic gear into a PM motor [50], as shown in Figure 14b, LSLT operation can be obtained. As compared to traditional PM motors, the magnetic-geared in-wheel motor offers higher torque density and less cogging torque [51], hence being more suitable for the in-wheel drive system than other motor topologies.
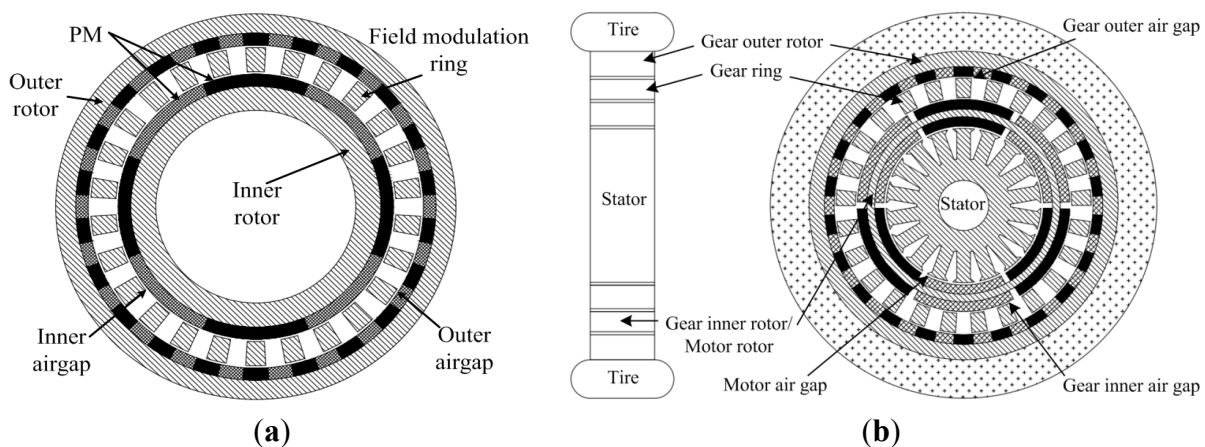

(a)   (b)

Figure 14. Magnetic gear. (**a**) Coaxial magnetic gear; (**b**) Magnetic-geared in-wheel motor.

However, the pure imitation of the traditional mechanical gear speed reduction element yields not only a waste of magnets, but also a complex structure. Furthermore, the existence of three airgaps reduces the torque density of the whole motor.

By replacing one of the two PM rotors in the coaxial magnetic gear with a stator equipped with armature windings, a more compact "magnetic-geared motor" can be achieved. The modulation effect of the field ring helps the interaction of the armature windings with the remaining PM rotor (this PM rotor usually has numerous poles). Since the field ring and the stator are both stationary, they can be constructed as a whole core, as shown in Figure 15. An expensive high-precision position sensor might be necessary for the control of the magnetic-geared motor due to the numerous poles of the PM rotor. Hence, a self-sensing control method is valuable for this type of motor [52]. An *ad hoc*-designed magnetic pole structure avoids the magnetic leakage due to the large pole number [53] and improves the utilization of the permanent magnets. From these advances, a magnetic-geared in-wheel drive system has become practical equipment for EV applications.
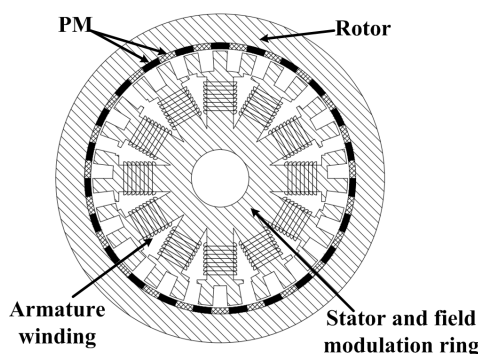

Figure 15. Magnetic-geared motor with a single airgap.

4.2. ISG System Based on the PM Motor

Traditional automotive applications usually use two independent machines for starting and generating. Although the structure is simple, the functions of the two motors cannot be fully utilized. Large volume and weight are not good news for vehicle applications. An integrated starter/generator (ISG) uses one machine, as shown in Figure 16, and has been a trend in the automotive industry [54,55].
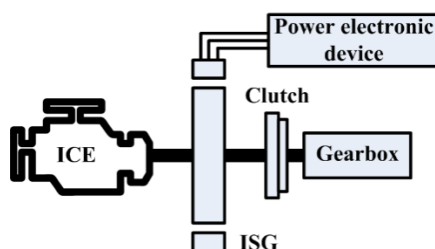

Figure 16. Hybrid power train with an integrated starter generator (ISG) system.

Since the rotor of the ISG directly connects to the ICE crankshaft and the maximum speed of the ICE can reach more than 6000 r/min, the ISG has to work at a very high speed as a generator. Hence, the flux weakening ability will be a challenge for the ISG. The hybrid-excitation stator-PM motors have excellent field regulation ability and a reliable structure. These features make them suitable for

the ISG application. As shown in Figure 17, a hybrid-excitation stator-PM motor is specifically designed for the ISG system [56]. In this prototype, the air bridge functions to amplify the effect of flux weakening when the field magnetomotive force (MMF) is opposing the PM flux.
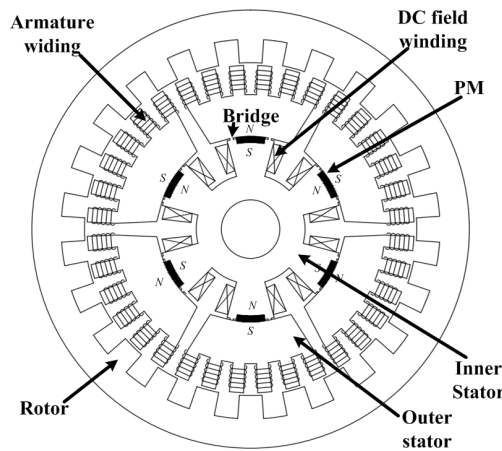

Figure 17. The hybrid-excitation stator-PM motor for the ISG system.

As previously mentioned, proper control of the positive and negative excitation current on DC field winding can adjust the PM flux directly, so that the output voltage can be regulated well and even remained unchanged. As shown in Figure 18, when the ISG works as a generator, flux regulation by the DC field winding makes the output voltage remain constant in a wide range of speed and load conditions. Hence, it sharply simplifies the design of the power electronic device.
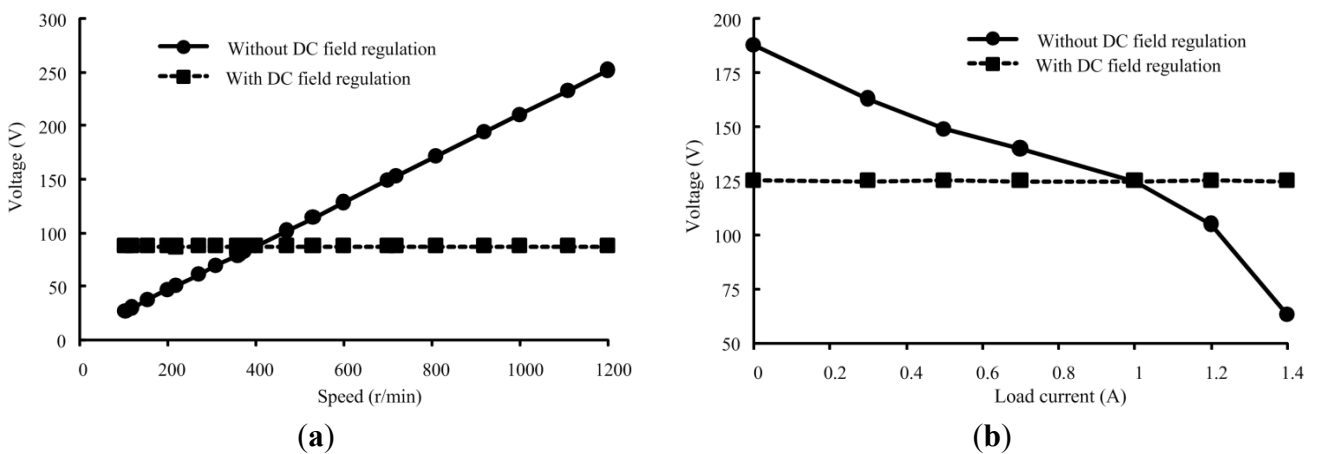

Figure 18. DC field regulation of the ISG (hybrid-excitation stator-PM motors). (**a**) Voltage *versus* speed; (**b**) Voltage *versus* load current.

5. Power Distribution System for an HEV

In the HEV application, the power required for the motor drive is mainly produced by the mechanical power of the ICE output. The current mainstream HEV powertrain solution is the so-called "series-parallel" system. Namely, the mechanical power of the ICE output can be split into two parts by a power split device: one part is transmitted to drive wheels directly; the other is converted to electric power by a generator to charge the battery or to support the traction motor and the vehicle

electrical load consumption. As the power split device can decouple the ICE crankshaft and the wheels' drive system, the ICE speed is able to be independent of the wheel speed. Hence, the ICE can work at its optimal operating point so as to enhance the fuel efficiency and minimize the emission.

Toyota used the planetary gear as the core of the HEV power split device (Toyota hybrid system (THS); shown as Figure 19), which has been applied in commercial HEV products successfully. Up to now, this successful industrial design has been recognized as a reference for automotive hybridization.
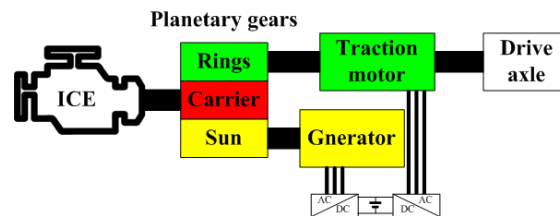

Figure 19. Schematic of the Toyota hybrid system (THS).

The rotation speeds of the three components in the planetary gear abide by:

$$n_{sun} + p \times n_{ring} = (1 + p) \times n_{carrier} \tag{2}$$

where n_{sun}, n_{ring} and $n_{carrier}$ are the rotation speeds of the sun gear, ring gear and the planets carrier, respectively, and p is a characteristic parameter, which can be considered as the transmission ratio. According to Equation (2), by adjusting the speed of the sun gear connected to the generator shaft, the transmission ratio between ICE speed and wheel speed can vary continuously. Hence, it is called the electric continuously-variable transmission (ECVT).

However, due to the innate drawbacks of mechanical gears, there are inevitable gear backlash, mechanical vibration and abrasion caused by the planetary gear in the THS. In recent years, replacing the THS by a complete electrified power split system has been considered as a promising research direction [57,58]. Three advanced solutions will be introduced as follows.

5.1. Dual-Rotor PM ECVT

Currently, the new ECVT system based on a dual-rotor motor has attracted increasing research attention. The dual-rotor motor can be made up of an IM motor [59] or PM motor [60]. Due to the merits of the PM motor mentioned in Section 2, PM motor is a better choice for the HEV application. Figure 20 shows the diagram of the ECVT system made of the dual-rotor PM motor. The inner rotor connects to the wheels, and the outer rotor connects to the ICE crankshaft. The mechanical power of the ICE output can be directly transmitted to the outer rotor or converted to electric power by the windings in the inner rotor and stator. The speed and torque of the outer rotor can be controlled by the windings in the inner rotor and stator; therefore, the drive shaft speed is independent of ICE. This decoupling effect makes the ICE always run in a high efficiency situation.
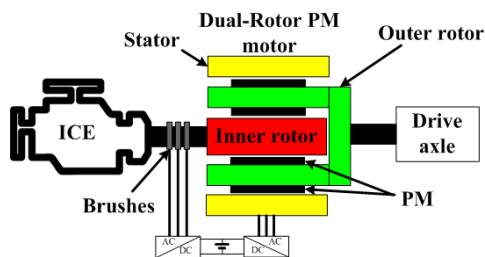
Figure 20. Dual-rotor PM electric continuously-variable transmission (ECVT).

The dual-rotor PM motor can be regarded as the cascade of the two PM motors (inner and outer motors), and the outer rotor provides yokes for both of the two PM motors. Through the reasonable design of the outer rotor yoke thickness, the coupling of the inner and outer air gap magnetic field can be sharply reduced. Consequently, the control algorithm of the dual-rotor PM motor can be simplified.

The main components of the dual-rotor PM motor are shown in Figure 21. The inner rotor is at the innermost position of the motor, which seriously impacts the heat dissipation of the inner rotor winding. Liquid cooling cannot be used for rotor winding, so the heating problem is the main difficulty for this ECVT system. To resolve the problem, a detailed thermal analysis is required for the dual-rotor PM motor to establish the copper loss and iron loss model [61]. On the base of the loss model, the temperature distribution of the whole motor can be calculated, through which a special type of forced air cooling system is designed to improve the heat dissipation of the dual-rotor PM motor [62,63].

Figure 21. Prototype of the dual-rotor PM motor.

For the inner air gap of the motor, since the PM rotor (outer rotor) and armature rotor (inner rotor) rotate at the same time and their speeds are different, position decoupling is the key to the control strategy and algorithm. Applying self-sensing control technology to the dual-rotor motor can reduce the cost of the ECVT system and improve the reliability of the control system [64]. The quantitative comparison of the fuel consumptions between the dual-rotor PM ECVT and the THS in [65] has shown that the dual-rotor PM ECVT can perform as well as the THS.

Although the structure of the dual-rotor PM motor system is compact and has the merit of being gearless, the slip rings and brushes in the inner rotor limit its application to a high power density system.

5.2. Dual-Stator PM Brushless ECVT

To overcome the disadvantage of the dual-rotor PM motor, a brushless ECVT system based on the dual-stator PM motor is proposed [66,67]. As shown in Figure 22, the whole brushless ECVT system needs two motors, namely the dual-stator motor on the left and the traction motor (induction motor) on

the right. The mechanical power from ICE is injected to the ECVT system by the double-layer PM rotor and split into two parts. The outer stator windings are used to generate the main power flow, which goes through the "direct power switch" or "rectifier-inverter path" to drive the traction motor. The inner stator windings are used to generate charging power flow for the battery, which goes through the "Rectifier 2path". This structure is similar to the series hybrid power system, namely none of the mechanical power from the ICE can be transmitted to the drive axle directly. The difference is that, through reasonable design, the frequency of the outer stator windings can be close to the frequency of the traction motor during high speed cruise mode. At this time, the main power flow can be directly transmitted to the traction motor by the "direct power switch", so as to avoid the loss of the power electronic devices [67].
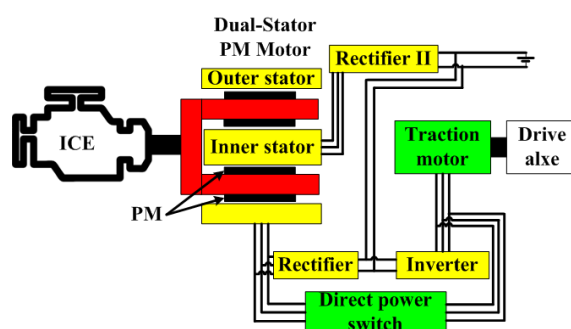

Figure 22. Dual-stator PM brushless ECVT.

Similar to the dual-rotor PM motor, the dual-stator PM motor can be regarded as the parallel of the two PM motors (inner and outer motors). Their dimensions determine the proportion of the power split. Based on the power-size equation of the two motors [68], their dimensions should be designed according to a balance between the split ratio optimization principle and the power split requirement of the actual application. Such a dual-stator PM motor design method has been reported in [68,69]. The prototype of the dual stator motor is shown in Figure 23.
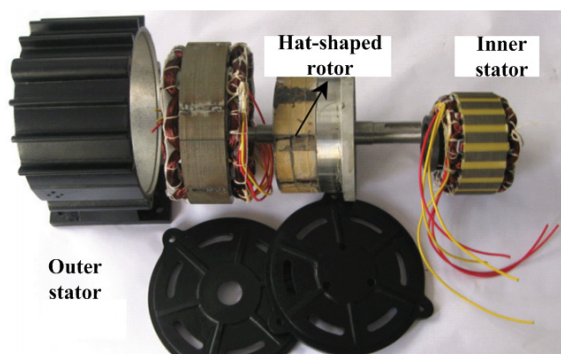

Figure 23. Prototype of the dual-stator PM motor.

5.3. Dual-Rotor Magnetic-Geared Brushless ECVT

When the field modulation ring of the coaxial magnetic gear in Figure 14a rotates, the magnetic-geared motor will transform to a new dual-rotor magnetic-geared motor (MGDRM), as shown in Figure 24.

Similar to Equation (1), the speeds of the three components in Figure 24 will comply with:

$$n_w + \frac{p_{ir}}{p_w} \times n_{ir} = \left(1 + \frac{p_{ir}}{p_w}\right) \times n_{or} \tag{3}$$

where n_{ir} and p_{ir} are the speed and pole pair number of the inner rotor (PM rotor), respectively; n_{or} and p_{or} are the speed and pole pair number of the outer rotor (field modulation ring), respectively; and n_w and p_w are the speed and pole pair number of the armature field, respectively. This relationship is very similar to Equation (2), which means that the MGDRM might be a potential replacement for the THS [70,71].
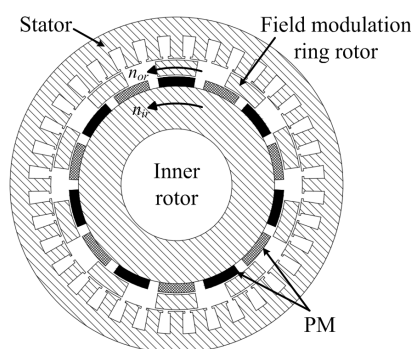

Figure 24. Structure of the magnetic-geared dual-rotor brushless machine (MGDRM).

Figure 25 shows a prototype of the MGDRM. In order to eliminate the asymmetry of the phase back-EMF waveforms and to suppress the cogging torque, a complementary structure has been proposed [72]. Based on the similarity between the coaxial magnetic gear and the planetary gear, the brushless ECVT system, which contains an MGDRM, can be achieved as shown in Figure 26. The mechanical power of the ICE output can be split into two parts by the MGDRM. Part of the mechanical power is directly transmitted to the drive axle by the inner rotor; the rest of the power is converted to electric power by the armature windings to support the traction motor and to charge the battery. Because vehicles have several complex operation patterns, such as regenerative braking mode and rapid acceleration mode, the output mechanical power flow and the electric power flow are bidirectional.
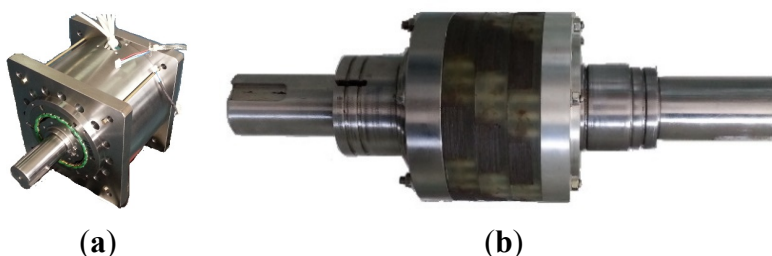

| (a) | (b) |

Figure 25. A prototype of the MGDRM: (**a**) Prototype; (**b**) Assembly of the inner and outer rotors.
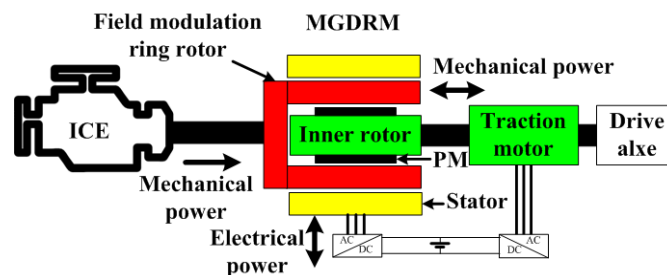
Figure 26. Dual-rotor magnetic-geared brushless ECVT.

The key features of the three ECVTs based on different motor topologies are summarized in Table 4.

Table 4. Comparison of different ECVT topologies.

ECVT topology	Dual-rotor PM	Dual-stator PM	Magnetic-geared
Stator number	1	2	1
Rotor number	2	1	2
Winding number	2	2	1
Brush	Yes	No	No
Converter number	2	4	2
Magnet amount	Low	High	Low
Copper amount	High	High	Low
Torque density	Medium	Medium	High

6. Conclusions and Developing Trends

In this paper, advanced solutions on electric machines and machine-based systems for the powertrain of EV/HEVs have been presented, with emphasis on the advanced PM motor topologies, including a stator permanent magnet (PM) motor, a hybrid-excitation motor, a flux memory motor, an in-wheel motor drive and an integrated starter/generator (ISG). Moreover, three machine-based power split devices for HEVs are expounded, built around the dual-rotor PM machine, the dual-stator PM brushless machine and the magnetic-geared dual-rotor machine, of which the one based on the magnetic-geared dual-rotor machine may be more promising due to the brushless and compact structure.

Innovation never stops. The development of electric drive technology for EV/HEVs may be implemented at four levels:

(i) Motor level: various novel motor topologies and control algorithm may be proposed to satisfy the specific requirements of EV motors.
(ii) Drive system level: a novel electric drive system with advanced performance should be developed to replace the mechanical gear and transmission axle by electric technology and to achieve the full electrification of the power train.
(iii) Powertrain level: the optimized design of the operation patterns for the electrified powertrain, especially for HEVs and plug-in HEVs with ECVT, to enhance the energy economy of the vehicles.
(iv) Whole vehicle level: to minimize the overall cost and weight of the vehicle, the motor drive system may be integrated with other electric devices. A motor drive system integrated with a charger for a plug-in HEV is just an example.

Acknowledgments

Author Contributions

Ming Cheng and Le Sun mainly drew up the review of the advanced electric machines and machine-based systems for EV and HEV. The manuscript was improved and revised by Giuseppe Buja and Lihua Song. All of the authors contributed to the paper writing.

Conflicts of Interest

The authors declare no conflict of interest.

References

1. Chan, C.C.; Chau, K.T. *Modern Electric Vehicle Technology*, 1st ed.; Oxford University Press: New York, NY, USA, 2001; pp. 16–28.
2. Cheng, M.; Chan, C.C. General requirement of traction motor drives. *Encycl. Automot. Eng.* **2015**, *3*, 1261–1278.
3. Chan, C.C.; Chau, K.T. An overview of power electronics in electric vehicles. *IEEE Trans. Ind. Electron.* **1997**, *44*, 3–13.
4. Zhu, Z.Q.; Howe, D. Electrical machines and drives for electric, hybrid, and fuel cell vehicles. *Proc. IEEE* **2007**, *95*, 746–765.
5. Dorrell, D.G.; Knight, A.M.; Popescu, M.; Evans, L.; Staton, D.A. Comparison of different motor design drives for hybrid electric vehicles. In Proceedings of the IEEE Energy Conversion Congress and Exposition (ECCE), Atlanta, GA, USA, 12–16 September 2010; pp. 3352–3359.
6. Cheng, M.; Hua, W.; Zhang, J.; Zhao, W. Overview of stator-permanent magnet brushless machines. *IEEE Trans. Ind. Electron.* **2011**, *58*, 5087–5101.
7. Liao, Y.; Liang, F.; Lipo, T.A. A novel permanent magnet machine with doubly salient structure. *IEEE Trans. Ind. Appl.* **1995**, *31*, 1069–1078.
8. Cheng, M.; Chau, K.T.; Chan, C.C. Static characteristics of a new doubly salient permanent magnet motor. *IEEE Trans. Energy Convers.* **2001**, *16*, 20–25.
9. Cheng, M.; Chau, K.T.; Chan, C.C. Design and analysis of a new doubly salient permanent magnet motor. *IEEE Trans. Magn.* **2001**, *37*, 3012–3020.
10. Zhang, J.; Cheng, M.; Chen, Z.; Hua, W. Comparison of stator-mounted permanent magnet machines based on a general power equation. *IEEE Trans. Energy Convers.* **2009**, *24*, 826–834.
11. Cheng, M.; Chau, K.T.; Chan, C.C.; Zhou, E.; Huang, X. Nonlinear varying-network magnetic circuit analysis for doubly salient permanent magnet motors. *IEEE Trans. Magn.* **2000**, *36*, 339–348.
12. Zhang, J.; Wang, M.; Cheng, M. Prediction of iron losses in doubly salient permanent magnet machine with rectangular current waveform. *J. Appl. Phys.* **2012**, *111*, 07E716.

13. Zhu, S.; Cheng, M.; Dong, J.; Du, J. Core loss analysis and calculation of stator permanent magnetmachine considering DC-biased magnetic induction. *IEEE Trans. Ind. Electron.* **2014**, *61*, 5203–5212.

14. Zhu, Z.Q.; Chen, J.T. Advanced flux-switching permanent magnet brushless machines. *IEEE Trans. Magn.* **2010**, *46*, 1447–1453.

15. Hua, W.; Cheng, M.; Zhu, Z.Q.; Howe, D. Analysis and optimization of back EMF waveform of a flux-switching permanent magnet motor. *IEEE Trans. Energy Convers.* **2008**, *23*, 727–733.

16. Hua, W.; Cheng, M. Cogging torque reduction of flux-switching permanent magnet machines without skewing. In Proceedings of the International Conference on Electrical Machines and Systems (ICEMS 2008), Wuhan, China, 17–20 October 2008; pp. 3020–3025.

17. Jia, H.; Cheng, M.; Hua, W.; Zhao, W.; Li, W. Torque ripple suppression in flux-switching PM motor by harmonic current injection based on voltage space-vector modulation. *IEEE Trans. Magn.* **2010**, *46*, 1527–1530.

18. Hua, W.; Cheng, M.; Zhu, Z.Q. Design of flux-switching permanent magnet machine considering the limitation of inverter and flux-weakening capability. In Proceedings of the Conference Record of the 2006 IEEE Industry Applications Conference (41st IAS Annual Meeting), Tampa, FL, USA, 8–12 October 2006; pp. 2403–2410.

19. Hua, W.; Zhang, G.; Cheng, M. Investigation and design of a high power flux-switching permanent magnet machine for hybrid electric vehicles. *IEEE Trans. Magn.* **2015**, *51*, 8201805, doi:10.1109/TMAG.2014.2345732.

20. Chen, J.T.; Zhu, Z.Q.; Iwasaki, S.; Deodhar, R.P. Influence of slot opening on optimal stator and rotor pole combination and electromagnetic performance of switched-flux PM brushless AC machines. *IEEE Trans. Ind. Appl.* **2011**, *47*, 1681–1691.

21. Chen, J.T.; Zhu, Z.Q. Influence of the rotor pole number on optimal parameters in flux-switching PM brushless AC machines by the lumped-parameter magnetic circuit model. *IEEE Trans. Ind. Appl.* **2010**, *46*, 1381–1388.

22. Chen, J.T.; Zhu, Z.Q. Winding configurations and optimal stator and rotor pole combination of flux-switching PM brushless AC machines. *IEEE Trans. Energy Convers.* **2010**, *25*, 293–302.

23. Zhang, G.; Cheng, M.; Hua, W. Analysis of flux-switching permanent magnet machine by nonlinear magnetic network model with bypass-bridges. In Proceedings of the 2010 International Conference on Electrical Machines and Systems (ICEMS), Incheon, Korea, 10–13 October 2010; pp. 1787–1791.

24. Cao, R.; Mi, C.; Cheng, M. Quantitative comparison of flux-switching permanent magnet motors with interior permanent magnet motor for EV, HEV, and PHEV applications. *IEEE Trans. Magn.* **2012**, *48*, 2374–2384.

25. Nalepa, R.; Kowalska, T.O. Optimum trajectory control of the current vector of a nonsalient-pole PMSM in the field-weakening region. *IEEE Trans. Ind. Electron.* **2012**, *59*, 2867–2876.

26. EL-Refaie, A.M.; Jahns, T.M. Optimal flux weakening in surface PM machines using fractional-slot concentrated windings. *IEEE Trans. Ind. Appl.* **2005**, *41*, 790–800.

27. Zhu, X.; Cheng, M.; Zhao, W.; Liu, C.; Chau, K.T. A transient cosimulation approach to performance analysis of hybrid excited doubly salient machine considering indirect field-circuit coupling. *IEEE Trans. Magn.* **2007**, *43*, 2558–2560.

28. Dong, G.; Cheng, M.; Hua, W. Modeling of a novel hybrid-excited flux-switching machine drives for hybrid electrical vehicles. In Proceedings of the 2010 International Conference on Electrical Machines and Systems (ICEMS), Incheon, Korea, 10–13 October 2010; pp. 839–843.

29. Zhu, X.; Cheng, M. Design analysis and control of hybrid excited doubly salient stator-permanent magnet motor. *Sci. China Technol. Sci.* **2010**, *53*, 188–199.

30. Shu, Y.; Cheng, M.; Kong, X. Online efficiency optimization of stator-doubly-fed doubly salient motor based on a loss model. In Proceedings of the International Conference on Electrical Machines and Systems (ICEMS 2008) Wuhan, China, 17–20 October 2008; pp. 1174–1178.

31. Hua, W.; Cheng, M.; Zhang, G. A novel hybrid excitation flux-switching motor for hybrid vehicles. *IEEE Trans. Magn.* **2009**, *45*, 4728–4731.

32. Wang, Y.; Deng, Z. Hybrid excitation topologies and control strategies of stator permanent magnet machines for DC power system. *IEEE Trans. Ind. Electron.* **2012**, *59*, 4601–4616.

33. Hua, W.; Zhang, G.; Cheng, M. Flux-regulation theories and principles of hybrid-excited flux-switching machines. *IEEE Trans. Ind. Electron.* **2015**, *62*, 5359–5369 .

34. Ostovic, V. Memory motors. *IEEE Ind. Appl. Mag.* **2003**, *9*, 52–61.

35. Gong, Y.; Chau, K.T.; Jiang, J.Z.; Yu, C.; Li, W. Analysis of doubly salient memory motors using Preisach theory. *IEEE Trans. Magn.* **2009**, *45*, 4676–4679.

36. Yu, C.; Chau, K.T. Design, analysis, and control of DC-excited memory motors. *IEEE Trans. Energy Convers.* **2011**, *26*, 479–489.

37. Yu, C.; Chau, K.T. Dual-mode operation of DC-excited memory motors under flux regulation. *IEEE Trans. Ind. Appl.* **2011**, *47*, 2031–2041.

38. Zhu, X.; Quan, L.; Chen, D.; Cheng, M.; Hua, W.; Sun, X. Electromagnetic performance analysis of a new stator-permanent magnet doubly salient flux memory motor using a piecewise-linear hysteresis model. *IEEE Trans. Magn.* **2011**, *47*, 1106–1109.

39. EL-Refaie, A.M. Fault-tolerant permanent magnet machines a review. *IET Electr. Power Appl.* **2011**, *5*, 59–74.

40. Zhao, W.; Cheng, M.; Zhu, X.; Hua, W.; Kong, X. Analysis of fault-tolerant performance of a doubly salient permanent magnet motor drive using transient cosimulation method. *IEEE Trans. Ind. Electron.* **2008**, *55*, 1739–1748.

41. Zhao, W.; Chau, K.T.; Cheng, M.; Ji, J.; Zhu, X. Remedial brushless AC operation of fault-tolerant doubly salient permanent magnet motor drives. *IEEE Trans. Ind. Electron.* **2010**, *57*, 2134–2141.

42. Zhao, W.; Cheng, M.; Hua, W.; Jia, H.; Cao, R. Back-EMF harmonic analysis and fault-tolerant control of flux-switching permanent magnet machine with redundancy. *IEEE Trans. Ind. Electron.* **2011**, *58*, 1926–1935.

43. Zhao, W.; Cheng, M.; Chau, K.T.; Cao, R.; Ji, J. Remedial injected-harmonic-current operation of redundant flux-switching permanent magnet motor drives. *IEEE Trans. Ind. Electron.* **2013**, *60*, 151–159.

44. Levi, E. Multiphase electric machines for variable-speed applications. *IEEE Trans. Ind. Electron.* **2008**, *55*, 1893–1909.

45. Levi, E. Advances in converter control and innovative exploitation of additional degrees of freedom for multiphase machines. *IEEE Trans. Ind. Electron.* **2015**, doi:10.1109/TIE.2015.2434999.

46. Li, F.; Hua, W.; Cheng, M.; Zhang, G. Analysis of fault tolerant control for a nine-phase flux-switching permanent magnet machine. *IEEE Trans. Magn.* **2014**, *50*, 1–4.

47. Yu, F.; Cheng, M.; Li, F.; Chau, K.T.; Huang, J.; Hua, W. Fault tolerant control of harmonic injected nine-phase flux switching permanent magnet motor drive system. In Proceedings of the 17th International Conference on Electrical Machines and Systems (ICEMS), Hangzhou, China, 22–25 October 2014; pp. 3117–3122.

48. Li, X.; Chau, K.T.; Cheng, M.; Kim, B.; Lorenz, R.D. Performance analysis of a flux-concentrating field-modulated permanent magnet machine for direct-drive applications. *IEEE Trans. Magn.* **2015**, *51*, 1334–1364.

49. Li, X.; Chau, K.T.; Cheng, M.; Hua, W. Comparison of magnetic-geared permanent magnet machines. *Prog. Electromagn. Res.* **2013**, *133*, 177–198.

50. Chau, K.T.; Zhang, D.; Jiang, J.Z.; Liu, C.; Zhang, Y. Design of a magnetic-geared outer-rotor permanent magnet brushless motor for electric vehicles. *IEEE Trans. Magn.* **2007**, *43*, 2504–2506.

51. Fu, W.N.; Ho, S.L. A quantitative comparative analysis of a novel flux-modulated permanent magnet motor for low-speed drive. *IEEE Trans. Magn.* **2010**, *46*, 127–134.

52. Fan, Y.; Zhang, L.; Cheng, M.; Chau, K.T. Sensorless SVPWM-FADTC of a new flux modulated permanent-magnet wheel motor based on a wide-speed sliding mode observer. *IEEE Trans. Ind. Electron.* **2015**, *62*, 3143–3151.

53. Fan, Y.; Zhang, L.; Huang, J.; Han, X. Design, analysis and sensorless control of a self-decelerating permanent- magnet in-wheel motor. *IEEE Trans. Ind. Electron.* **2014**, *61*, 5788–5797.

54. Chau, K.T.; Chan, C.C. Emerging energy-efficient technologies for hybrid electric vehicles. *Proc. IEEE* **2007**, *95*, 821–835.

55. Wang, J.; Xia, Z.P.; Howe, D. Three-phase modular permanent magnet brushless machine for torque boosting on a downsized ICE vehicle. *IEEE Trans. Veh. Technol.* **2005**, *54*, 809–816.

56. Liu, C.; Chau, K.T.; Jiang, J.Z. A permanent magnet hybrid brushless integrated starter-generator for hybrid electric vehicles. *IEEE Trans. Ind. Electron.* **2010**, *57*, 4055–4064.

57. Cheng, Y.; Cheng, M. EVT and E-CVT for full hybrid electric vehicles. *Encycl. Automot. Eng.* **2015**, *3*, 1115–1123.

58. Bertoluzzo, M.; Bolognesi, P.; Buja, G.; Thakura, P. Role and technology of the power split apparatus in hybrid electric vehicles. In Proceedings of the 33rd Annual Conference of the IEEE Industrial Electronics Society (IECON 2007), Taipei, Taiwan, 5–8 November 2007; pp. 256–261.

59. Hoeijmakers, M.J.; Rondel, R. The electrical variable transmission in a city bus. In Proceedings of the 2004 IEEE 35th Annual Power Electronics Specialists Conference (PESC 04), Aachen, Germany, 20–25 June 2004; pp. 2773–2778.

60. Xu, L.; Zhang, Y.; Wen, X. Multioperational modes and control strategies of dual-mechanical-port machine for hybrid electrical vehicles. *IEEE Trans. Magn.* **2009**, *45*, 747–745.

61. Sun, X.; Cheng, M. Thermal analysis and cooling system design of dual mechanical port machine for wind power application. *IEEE Trans. Ind. Electron.* **2013**, *60*, 1724–1733.

62. Zheng, P.; Liu, R.; Thelin, P.; Nordlund, E.; Sadarangani, C. Research on the cooling system of a 4QT prototype machine used for HEV. *IEEE Trans. Energy Convers.* **2008**, *23*, 61–67.

63. Sun, X.; Cheng, M.; Zhu, S.; Zhang, J. Coupled electromagnetic-thermal-mechanical analysis for accurate prediction of dual-mechanical-port machine performance. *IEEE Trans. Ind. Appl.* **2012**, *48*, 2240–2248.

64. Zhu, Y.; Cheng, M.; Hua W.; Zhang, B. Sensorless control strategy of electrical variable transmission machines for wind energy conversion systems. *IEEE Trans. Magn.* **2013**, *49*, 3383–3386.

65. Vinot, E.; Cheng, Y.; Bouscayrol, A.; Reinbold, V. Improvement of an EVT-Based HEV using dynamic programming. *IEEE Trans. Veh. Technol.* **2014**, *63*, 40–50.

66. Wang, Y.; Cheng, M.; Chau, K.T. Review of electronic-continuously variable transmission propulsion system for full hybrid electric vehicles. *J. Asian Electric Veh.* **2009**, *7*, 1297–1302.

67. Wang, Y.; Cheng, M.; Fan, Y.; Chau, K.T. A double-stator permanent magnet brushless machine system for electric variable transmission in hybrid electric vehicles. In Proceedings of the 2010 IEEE Vehicle Power and Propulsion Conference (VPPC), Lille, France, 1–3 September 2010; pp. 1–5.

68. Wang, Y.; Cheng, M.; Chen, M.; Du, Y.; Chau, K.T. Design of high-torque-density double-stator permanent magnet brushless motors. *IET Electr. Power Appl.* **2011**, *5*, 317–323.

69. Wang, Y.; Cheng, M.; Fan, Y.; Chau, K.T. Design and analysis of double-stator permanent magnet brushless motor for hybrid electric vehicles. In Proceedings of International Conference on the Electrical Machines and Systems (ICEMS 2008), Wuhan, China, 17–20 October 2008; pp. 3241–3246.

70. Zheng, P.; Bai, J.; Tong, C.; Sui, Y.; Song, Z.; Zhao, Q. Investigation of a novel radial magnetic-field-modulated brushless double-rotor machine used for HEVs. *IEEE Trans. Magn.* **2013**, *49*, 1231–1241.

71. Bai, J.; Zheng, P.; Tong, C.; Song, Z.; Zhao, Q. Characteristic analysis and verification of the magnetic-field modulated brushless double-rotor machine. *IEEE Trans. Ind. Electron.* **2015**, *62*, 4023–4033.

72. Sun, L.; Cheng, M.; Jia, H. Analysis of a novel magnetic-geared dual-rotor motor with complementary structure. *IEEE Trans. Ind. Electron.* **2015**, doi:10.1109/TIE.2015.2437361.